Nuclear Physics B (Proc. Suppl.) 2 (1987) 179-190
North-Holland, Amsterdam

Fluid Mixing and Dynamical Systems

A. Leonard,* V. Rom-Kedar** and S. Wiggins**

*Aeronautics and **Applied Mathematics, California
Institute of Technology, Pasadena, California, 91125

1. INTRODUCTION

We consider problems of mixing in fluid flows and show how the methods of dynamical systems may be used in the analysis of these problems. In particular, we consider the problem of passive scalar mixing in incompressible fluid flows and decompose the problem into three stages as follows. The first problem is to express the desired quantities (reactant consumption rate, ...) in terms of statistics or functionals of the flow field $\mathbf{u}(\mathbf{x}, t)$. The second is to compute the flow field (or a sufficiently accurate characterization of it) and, the third, determine the desired statistical properties.

The third stage in this process can be formidable with no general solutions available except for the simplest two-dimensional steady flows. The problem is directly related to the fact that particle motion in two-dimensional unsteady fluids or even in three-dimensional steady flows can be chaotic, leading to good mixing but to major difficulties in analysis. On the other hand, we show that the techniques from the theory dynamical systems provide some hope for problems involving chaotic motion.

We illustrate the first stage in the process by studying in Section 2 the specific example of a simple diffusion flame with fast chemical kinetics in an arbitrary three-dimensional flow. We follow closely Ottino's analysis[1] of mixing of diffusing and reacting fluids. As might be expected the history of the local stretching of the flame sheet governs the local reactant consumption rate. By choosing the steady two-dimensional velocity field of a vortex we complete stages two and three of the analysis in Section 3 and recover the results of Marble[2] for the growth of the reacted core region. Mixing is poor. Flame sheets are stretched asymptotically only linearly in time by this flow.

In Section 4 we consider the flow induced by a pair of translating point vortices. In a frame moving with the pair the motion is again steady and produces only linear stretch rates. However if the pair is subjected to a time-periodic potential flow, chaotic particle motion can result with consequent dramatic increase in mixing. A complete theory of the diffusion flame problem is not possible at this time but we study this flow by performing numerical

0920–5632/87/$03.50

experiments and make a partial analysis of the problem for small perturbations by the method of Melnikov. In particular the Melnikov method allows us to prove analytically the existence of chaotic particle motions of the Smale horseshoe type and it gives an estimate of the extent of the "turbulent" or mixing zone in the neighborhood of the vortex pair and the rate at which unmixed fluid is brought into this zone.

Previous investigations of fluid mixing or chaotic particle motion that have employed concepts or techniques from dynamical systems theory include Aref's investigation[3] of a model flow system consisting of two "blinking" vortices, a further analysis of the same flow and another unsteady, two-dimensional model flow with alternating strain and rotation by Khakhar, et al[4] and the study of chaotic streamlines in certain steady three-dimensional Euler flows, known as Arnold-Beltrami-Childress (ABC) flows, by Dombre, et al[5].

2. FLAME SHEET - GENERAL ANALYSIS

Consider a flame sheet separating two reactants A and B. The stoichiometry of the reaction is such that equal masses of each reactant are consumed at the infinitely thin reaction zone on the flame sheet. A material point $\mathbf{p}$ on the sheet moves with velocity

$$\frac{d\mathbf{p}}{dt} = \mathbf{u}(\mathbf{p}, t) \tag{2.1}$$

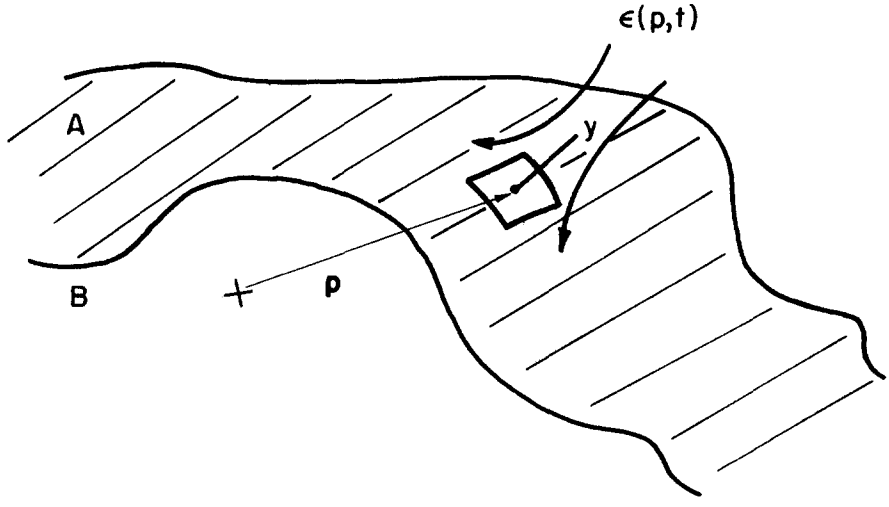

Fig. 1. Flame sheet geometry.

Let y be a relative coordinate normal to the sheet at $\mathbf{p}$ into the space containing A. For a thin flame we require only the first term in the Taylor series for the relative convection velocity in the direction normal to the flame sheet:

$$\mathbf{u}(\mathbf{x}, t) \cdot \mathbf{n} \sim \mathbf{u}(\mathbf{p}, t) \cdot \mathbf{n} - \varepsilon(\mathbf{p}, t) y \tag{2.2}$$

where ε is the (negative) strain rate normal to the sheet or, equivalently, the stretching rate of the sheet at $\mathbf{p}$. See Fig. 1. Thus the conservation equation for the mass fraction of reactant A, $\Phi_A(\mathbf{p}, y, t)$ is

$$\frac{\partial \Phi_A}{\partial t} - \varepsilon y \frac{\partial \Phi_A}{\partial y} = D \frac{\partial^2 \Phi_A}{\partial y^2} \tag{2.3}$$

where D is the diffusion coefficient. This problem may be transformed into the familiar diffusion equation, [1,2]

$$\frac{\partial \Phi_A}{\partial \tau} = D \frac{\partial^2 \Phi_A}{\partial \bar{y}^2} \tag{2.4}$$

by transforming to the material coordinate

$$\bar{y} = S(\mathbf{p}, t) y \tag{2.5}$$

and transforming in time according to

$$\tau = \int_0^t S^2(\mathbf{p}, t')\, dt' \tag{2.6}$$

where S is the fractional increase in sheet surface area at $\mathbf{p}$ given by

$$S(\mathbf{p}, t) = \exp\left[\int_0^t \varepsilon(\mathbf{p}, t')\, dt' \right] \tag{2.7}$$

Solving (2.4) we find that

$$\Phi_A(\mathbf{p}, y, t) = erf\left[\frac{Sy}{(4D\tau)^{1/2}} \right] \tag{2.8}$$

Thus the reactant consumption rate per unit initial area at $\mathbf{p}$, $C(\mathbf{p}, t)$, is given by

$$C(\mathbf{p}, t) = D\frac{\partial \Phi_A}{\partial y}\Big|_{y=0} S = \left[\frac{D}{\pi\tau}\right]^{1/2} S^2 \tag{2.9}$$

and the volume of reactant consumed per unit initial area is

$$V(\mathbf{p}, t) = \int_0^t C(\mathbf{p}, t')\, dt' = \left[\frac{4D\tau}{\pi}\right]^{1/2} \tag{2.10}$$

Except for the important proviso to be discussed below, the local time-dependent reactant consumption rate is completely determined in terms of the local stretch history of the flame sheet. The total product volume is then simply related to the average value of $V(\mathbf{p}, t)$ over the flame sheet but the distribution of stretch histories for a given flow are generally not known.

Furthermore the results cited are only valid up to the point when the zone of the product at $\mathbf{p}$ ($|y| < (4D\tau/S^2)^{1/2}$) "collides" with the product zone of another point on the sheet. See Fig. 2. Thus factoring in this sort of information for a general flow presents an even higher level of difficulty. The problem is reminiscent of the self-avoiding random walk.

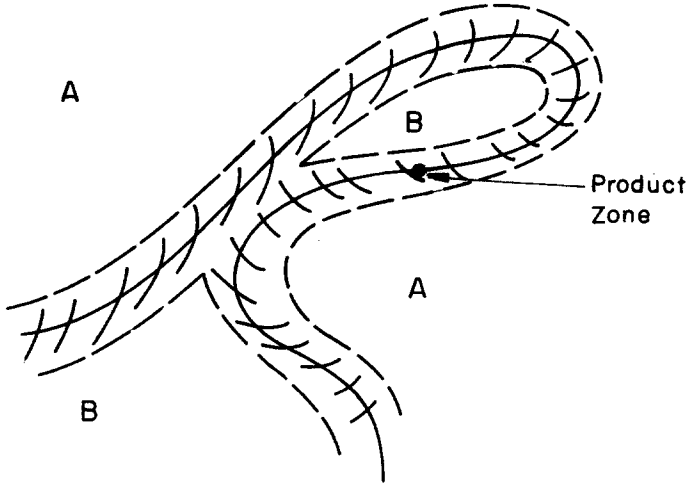

Fig. 2. Overlapping of product zones.

3. Spiral Flame Sheet

As an application of the above results we consider a single vortex with circulation Γ on an initially planar interface separating the two reactants. See Fig. 3. A surface element at a distance r from the vortex will rotate around the vortex with speed

$$v_\theta = \frac{\Gamma}{2\pi r} \tag{3.1}$$

if r is outside the vortex core. We find easily that this surface element is strained by the amount

$$S \to \frac{\Gamma t}{\pi r^2} \tag{3.2}$$

as $t \to \infty$ so that $\varepsilon \to 1/t$. The time τ is therefore given by (2.6),

$$\tau(r, t) \to \frac{\Gamma^2}{\pi^2 r^4} \frac{t^3}{3} \tag{3.3}$$

and the volume of reactant consumed per unit initial area is

$$V(r, t) \to \frac{\Gamma}{\pi r^2} \left[\frac{4Dt^3}{3\pi} \right]^{1/2} \tag{3.4}$$

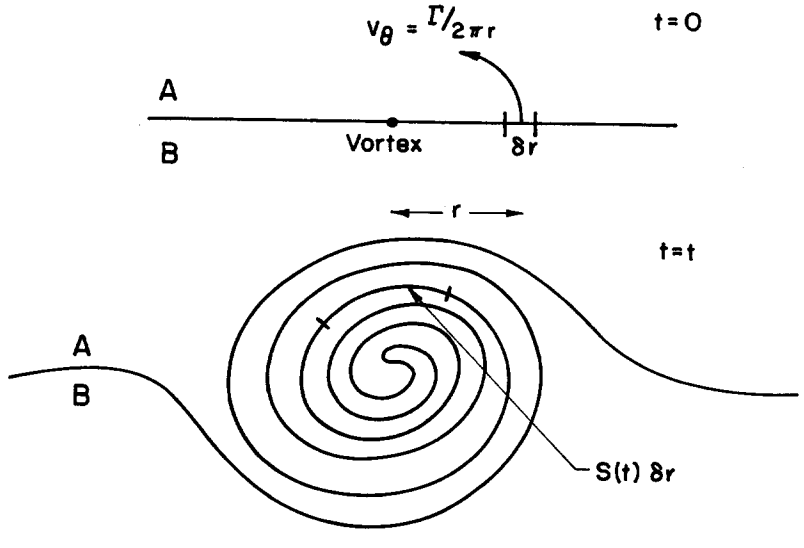

Fig. 3. Flame sheet in the flow of a single vortex. Time = 0 and a later time.

Again this result is only valid up to the point when the product zones collide or, in this case, when the reactants are consumed. Let $r^*(t)$ be the radius of the product core at time t. Then πr^* is the product volume per initial sheet area and hence the condition for product zone overlap is

$$V(r^*, t) = \frac{\pi r^*}{2} \tag{3.5}$$

which, using (3.4), gives

$$r^* \to \left[\frac{16}{3\pi^5}\right]^{1/6} D^{1/6}\Gamma^{1/3}t^{1/2} \tag{3.6}$$

in agreement with Marble[2].

Thus we have solved completely a simple combustion problem. On the other hand the flow was steady and two-dimensional resulting in only a linear increase in time of the flame sheet and relatively poor mixing. In our next example we consider the flow induced by a pair of translating point vortices. In a frame moving with the vortices the motion is steady so again we expect only linear stretching with time. However if the vortices are subjected to a time-dependent strain field a much more interesting flow results.

4. TRANSLATING POINT VORTICES

The fluid flow induced by a pair of translating point vortices separated by a distance $2d$ and with circulation $\pm\Gamma$ is sketched in Fig. 4. The motion is viewed in a frame moving with the velocity of the vorticies, $\mathbf{v} = \Gamma/4\pi d\ \hat{e}_x$. Again mixing would be poor as the stretching of any interface would be at most linear in t. In fact all the fluid inside the streamlines, ψ_{0+} and ψ_{0-}, connecting the front and rear stagnation points remains trapped, travelling with the vortices.

The stream function for this flow is

$$\psi_0 = -\frac{\Gamma}{4\pi}\log\left[\frac{(x-x_v)^2+(y-y_v)^2}{(x-x_v)^2+(y+y_v)^2}\right] - \frac{\Gamma y}{4\pi d} \tag{4.1}$$

where (x_v, y_v) is the position of the vortex in the upper half plane. For the unperturbed case, $(x_v, y_v) = (0, d)$, and the equations of particle motion are

$$\frac{dx}{dt} = \frac{\partial\psi_0}{\partial y}, \quad \frac{dy}{dt} = -\frac{\partial\psi_0}{\partial x} \tag{4.2}$$

and the three streamlines connecting the stagnation points are defined by

$$\psi_0(x, y) = 0 \qquad |x| \leq \sqrt{3}\, d \tag{4.3}$$

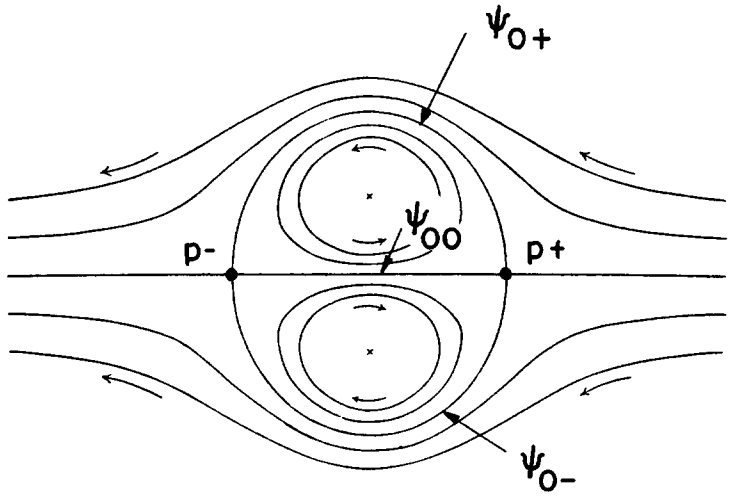

Fig. 4. Fluid induced by a pair of translating vortices. Unperturbed case.

Next we consider the effect of adding a time-periodic potential flow, i.e.,

$$\psi = \psi_0 + \psi_\varepsilon \tag{4.4}$$

with

$$\psi_\varepsilon = \varepsilon x y\, \omega \sin \omega t + v_\varepsilon y \tag{4.5}$$

and where the constant translation speed v_ε is included in anticipation of a coordinate change and is determined by requiring that the vortices have zero drift velocity. Such a flow satisfies the Euler equations and is produced, for example, by the motion of a vortex pair in a wavy-walled channel. The resulting motion of the vortices is relatively simple. Introducing the dimensionless parameter,

$$a = \frac{\Gamma}{2\pi\omega d^2} \tag{4.6}$$

and the dimensionless variables $(x/d, y/d) \to (x, y)$, $\omega t \to t$ and $v_\varepsilon/d\omega \to v_\varepsilon$, we compute the motion of the vortices with $(x_v(0), y_v(0)) = (0, 1)$ to obtain

$$x_\nu(t) = \exp(-\varepsilon \cos \omega t) \int_0^t \exp(\varepsilon \cos \omega t') \left\{ \frac{a}{2} [\exp(-\varepsilon(\cos \omega t' - 1)) - 1] + \nu_\varepsilon \right\} dt'$$

$$y_\nu(t) = \exp(\varepsilon(\cos \omega t - 1)) \tag{4.7}$$

where

$$\nu_\varepsilon = \frac{a}{2}\left[1 - \frac{\exp(\varepsilon)}{I_0(\varepsilon)}\right]$$

However our primary interest is in the motion of passive particles and, as we will see, this motion can be quite complicated. We give now only preliminary results of an analyis of the flow using methods of dynamical systems theory and of numerical experiments. A complete discussion of the results is forthcoming. The numerical experiments described below are based on the full equations of motion, valid for arbitrary ε , i.e. ,

$$\frac{dx}{dt} = \frac{\partial \psi}{\partial y}, \quad \frac{dy}{dt} = -\frac{\partial \Psi}{\partial x} \tag{4.8}$$

with the exact $\mathbf{x}_\nu = (x_\nu(t, \varepsilon, a), y_\nu(t, \varepsilon))$ in ψ_0. Our methods of analysis require the expansion of the right hand sides of (4.8) in powers of ε. The required expansions are simply done to obtain

$$\frac{dx}{dt} = a f_1(x, y) + \varepsilon g_1(x, y, t; a) + O(\varepsilon^2) \tag{4.9}$$

$$\frac{dy}{dt} = a f_2(x, y) + \varepsilon g_2(x, y, t; a) + O(\varepsilon^2)$$

where the functions g_1 and g_2 are periodic in t with period 2π.

The analysis focusses on the study of the Poincare map for the system (4.9),

$$P : (x(t_0),\ y(t_0) \rightarrow (x(t_0+2\pi),\ y(t_0+2\pi))$$

where t_0 is the section time for the map. For $\varepsilon = 0$ the streamlines of the flow shown in Fig. 4 are the invariant curves of the map. In particular, this map has two hyperbolic saddle points at

$$p_\pm = (\pm \sqrt{3}, 0)$$

and the unstable manifold of p_+ coincides with the stable manifold of p_-. These manifolds are also heteroclinic orbits and are defined by the streamlines $\psi_0\pm$ defined above in dimensional form.

For ε nonzero but small, these saddle points, along with their stable and unstable manifolds, persist and we can use the method of Melnikov[6] to test for a transversal intersection of the manifolds and hence chaotic particle motion. The signed distance between the manifolds is given by

$$d(t_0) = \frac{\varepsilon M(t_0)}{|\mathbf{f}(\mathbf{q}(-t_0))|} + O(\varepsilon^2) \tag{4.10}$$

where $\mathbf{f}$ and $\mathbf{q}$ are velocity and position on the unperturbed heteroclinic orbit, t_0 parameterizes the orbit and $M(t_0)$ is the Melnikov function given by

$$M(t_0) = \int_{-\infty}^{\infty} (f_1 g_2 - f_2 g_1)|_{q(t-t_0)} dt \tag{4.11}$$

We find that

$$M(t_0) = F(a) \sin t_0 \tag{4.12}$$

where $F(a)$ is shown in Fig. 5. Let a^* be the nonzero value of a such that $F(a^*) = 0$. (We find that $a^* \sim 1.78$.) Then if $a > 0, a \neq a^*$ the Melnikov function has simple zeroes in t_0 and therefore we have a transversal intersection of the stable and unstable manifolds. This implies the existence of Smale horsehoes and their attendent chaotic dynamics.

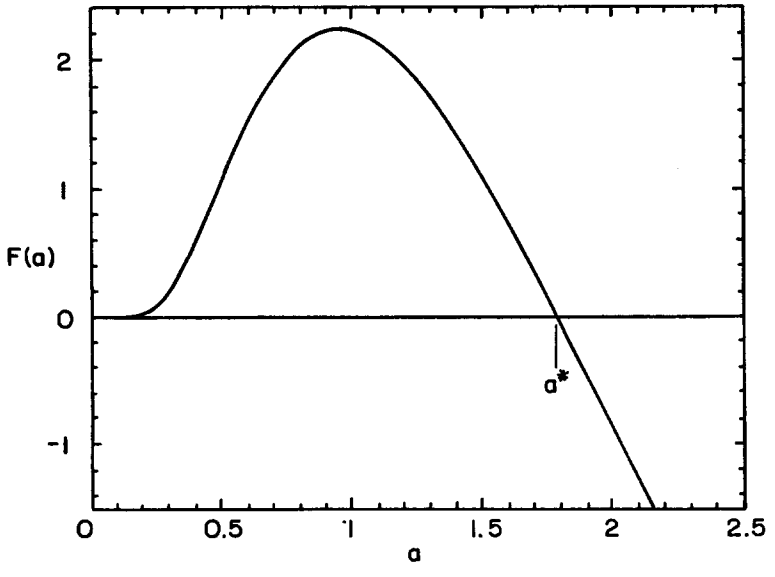

Fig. 5. Function from the Melnikov analysis.

But the analysis provides much more than just the fact that chaotic particle paths exist. From $M(t_0)$ we can compute $d(t_0)$ and therefore we can estimate the width of the "turbulent" zone around the unperturbed heteroclinic orbits. See Fig. 6. Only the fluid between the two dashed curves in Fig. 6 can be entrained, mixed and detrained. The inner dashed curve represents the Poincare section of the last KAM tori. Thus fluid inside of that curve never escapes from the inner zone. We find also the area of each of the "lobes" or regions bounded by the stable and unstable manifolds is given by

$$A = 2\varepsilon |F(a)| + 0(\varepsilon^2)$$

and this is precisely the volume or area of fluid that is entrained into the mixing zone per period, i.e. lobe A_0 maps to lobe A_1 in one period and then to A_2, A_3, etc. Of course an equal volume is ejected each period, namely lobe B_{-1} is mapped to B_0 and then to B_1, B_2, etc. Furthermore, from Fig. 5 the Melnikov analysis predicts that the width of the turbulent zone and the lobe area will at first increase with increasing parameter a, reach a maximum, go to zero at $a \sim a^*$ then increase again for $a > a^*$ but with a change in structure because $F(a)$ is now negative. (Recall that signed distance between the stable and unstable manifolds, $d(t_0)$, is proportional to $F(a)$.) Numerical computations for the stable and unstable manifolds of p_- and p_+, respectively, confirm these predictions and some examples are presented in Fig. 7.

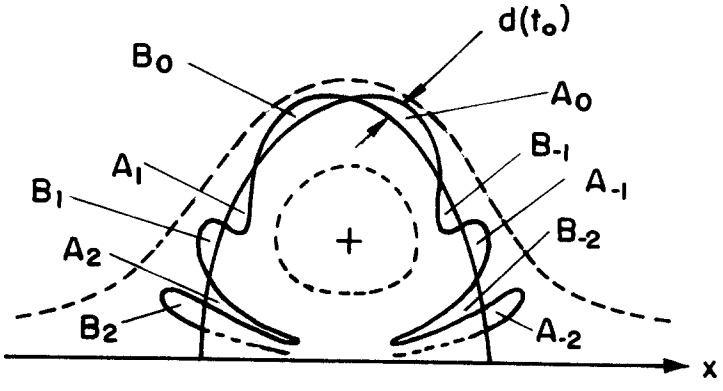

Fig. 6. Sketch of stable and unstable manifolds defining the lobe structures, the distance between manifolds, $d(t_0)$ and the boundaries of the mixing zone.

(a) $a = 0.3, \varepsilon = 0.1$

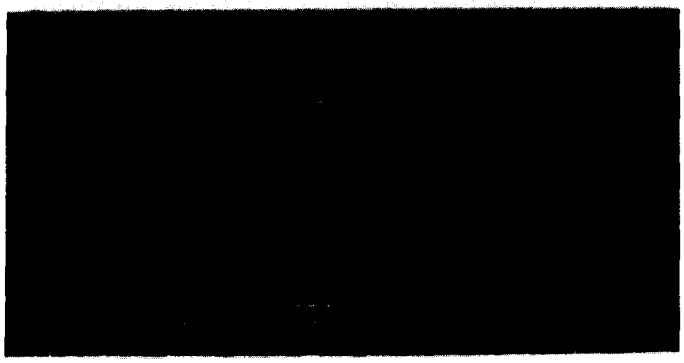

(b) $a = 0.7, \varepsilon = 0.1$

(c) $a = 1.48, \varepsilon = 0.1$

Fig. 7. Stable and unstable manifolds computed using the full equations

A number of interesting questions remain to be answered. At the present time we are investigating particle escape rates and the structure of the "escape" map. For example, we know that all particles in lobe A_0 are entrained into the interior in one period but what fraction of those escapes, i. e. arrives in B_0 after exactly k periods, and what is the distribution of those k-period particles in A_0 ?. With information of this kind we may begin to bridge the gap between the general analysis of the mixing problem presented in Section 2 and the application of that analysis to flows with chaotic particle motion.

5. SUMMARY

We have discussed several aspects of mixing in fluid flows, first by concentrating on a specific mixing problem - that of a simple diffusion flame with fast chemical kinetics in an arbitrary flow. The dependence of the local reactant consumption rate on the history of the local stretching of the flame sheet was determined up to the point where the flame sheet folds over on itself and the product zones collide. The analysis was applied to a simple, steady vortex flow producing a spiral flame sheet. In this case, the specific mixing problem is completely solved. Next we considered the flow due to a pair of translating point vortices subjected to a time-periodic potential flow. In this flow fluid is continually entrained into and detrained from a "turbulent" zone that moves with the translating pair. The original mixing problem was not solved but a considerable amount of information about entrainment rates, size of the mixing zone, etc., was obtained by using concepts and techniques from dynamical systems theory. In addition good insights into the mixing process were obtained. In particular, it was shown how the simple lobe structures of the stable and stable manifolds, with their ordered behavior under the Poincare' map, are responsible for chaotic mixing and mass transport.

ACKNOWLEDGEMENT - This work was partially supported by the Office of Naval Research contract N000 14-85-K-0205.

6. References

1) J. M. Ottino, J. Fluid Mech. 114 (1982) 83.

2) F. E. Marble, Growth of a Diffusion Flame in the Field of a Vortex, in: Recent Advances in the Aerospace Sciences, ed. C. Casci (Plenum Publishing, 1985) pp. 395-413.

3) H. Aref, J. Fluid Mech. 143 (1984) 1.

4) D. V. Khakhar, H. Rising and J. M. Ottino, J. Fluid Mech. 172 (1986) 419.

5) T. Dombre, U. Frisch, J. M. Greene, M. Henon, A. Mehr and A. M. Soward, J. Fluid Mech 167 (1986) 353.

6) J. Guckenheimer and P. Holmes, Nonlinear Oscillations, Dynamical Systems, and Bifurcations of Vector Fields (Springer-Verlag, New York, 1983).